Published OnlineFirst January 20, 2017; DOI: 10.1158/1078-0432.CCR-16-2745

Clinical Cancer Research

Bombesin Antagonist-Based Radiotherapy of Prostate Cancer Combined with WST-11 Vascular Targeted Photodynamic Therapy

Kwanghee Kim[1], Hanwen Zhang[2], Stephen La Rosa[1], Sylvia Jebiwott[1], Pooja Desai[2], Simon Kimm[3], Avigdor Scherz[4], Joseph A. O'Donoghue[5], Wolfgang A. Weber[6], and Jonathan A. Coleman[7]

Abstract

Purpose: DOTA-AR, a bombesin-antagonist peptide, has potential clinical application for targeted imaging and therapy in gastrin-releasing peptide receptor (GRPr)–positive malignancies when conjugated with a radioisotope such as ^{90}Y. This therapeutic potential is limited by the fast washout of the conjugates from the target tumors. WST-11 (Weizmann STeba-11 drug; a negatively charged water-soluble palladium-bacteriochlorophyll derivative, Tookad Soluble) vascular targeted photodynamic therapy (VTP) is a local ablation approach recently approved for use in early-stage prostate cancer. It generates reactive oxygen/nitrogen species within tumor blood vessels, resulting in their instantaneous destruction followed by rapid tumor necrosis. We hypothesize that the instantaneous arrest of tumor vasculature may provide a means to trap radiopharmaceuticals within the tumor, thereby improving the efficacy of targeted radiotherapy.

Experimental Design: GRPr-positive prostate cancer xenografts (PC-3 and VCaP) were treated with ^{90}Y-DOTA-AR with or without VTP. The uptake of radioisotopes was monitored by Cherenkov luminescence imaging (CLI). The therapeutic efficacy of the combined VTP and ^{90}Y-DOTA-AR in PC-3 xenografts was assessed.

Results: CLI of ^{90}Y-DOTA-AR demonstrated longer retention of radiotracer within the VTP-treated PC-3 xenografts compared with the non–VTP-treated ones ($P < 0.05$) at all time points (24–144 hours) after ^{90}Y-DOTA-AR injection. A similar pattern of retention was observed in VCaP xenografts. When ^{90}Y-DOTA-AR administration was combined with VTP, tumor growth delay was significantly longer than for the control or the monotherapy groups.

Conclusions: Tumor vascular arrest by VTP improves ^{90}Y-DOTA-AR retention in the tumor microenvironment thereby enhancing therapeutic efficacy. *Clin Cancer Res; 1–9. ©2017 AACR.*

Introduction

Targeted imaging and radionuclide-based therapeutics have shown great promise for noninvasive clinical applications in cancers expressing specific biomarkers, especially those that are associated with key biologic functions such as mitogenesis, neoangiogenesis, and cell migration. Several radiolabeled monoclonal antibodies and bioactive small peptides have been developed to bind with high specificity to such biomarkers and tested for clinical utility. However, the therapeutic window is favorable only when the radiotracer remains in high concentrations within the environment of the targeted cancer cells and rapidly cleared from the circulation and normal organs. Radiolabeled peptides can be favorable in this regard, as they can quickly diffuse into target cells and while clearing rapidly from circulation or nonspecific tissues with less immunogenicity compared with the radiolabeled monoclonal antibodies, resulting in high image contrast at early time points (1). However, uptake of radiopeptides in target cell populations is relatively "low," and the majority of administrated radiopeptides undergoes urinary excretion within 1 hour. Consequently, a large dose of radiopeptide is used to improve efficacy of radionuclide-based therapeutics (2, 3). The short dwell time of radiolabeled peptide within the target cells further limits the treatment efficacy of single-dose regimens. These limitations have led to extensive efforts in looking for novel means to extend the residence of radioisotopes used as beta and alpha emitters in the tumor microenvironment.

While numerous studies aim at improving the tumor affinity of the radiotracer conjugates, we sought to provide a means for trapping radiotracers within the tumor microenvironment by utilizing WST-11 vascular targeted photodynamic (VTP) therapy, a novel form of tissue treatment produced by a class of photosensitizing agents derived from bacteriochlorophyll.

[1]Department of Surgery, Memorial Sloan Kettering Cancer Center, New York. [2]Radiochemistry and Imaging Sciences Service, Department of Radiology, Memorial Sloan Kettering Cancer Center, New York. [3]Urology, Palo Alto Medical Foundation, Stanford, California. [4]Plant Science, Weizmann Institute of Science, Rehovot, Israel. [5]Department of Medical Physics, Memorial Sloan Kettering Cancer Center, New York. [6]Molecular Imaging and Therapy Services, Department of Radiology, Memorial Sloan Kettering Cancer Center, New York. [7]Division of Urology, Department of Surgery, Memorial Sloan Kettering Cancer Center, New York.

Note: Supplementary data for this article are available at Clinical Cancer Research Online (http://clincancerres.aacrjournals.org/).

K. Kim and H. Zhang contributed equally to this study.

Corresponding Author: Jonathan A. Coleman, Division of Urology, Department of Surgery, Memorial Sloan Kettering Cancer Center, New York, NY 10065. Phone: 646-422-4432; E-mail: colemanj@mskcc.org

doi: 10.1158/1078-0432.CCR-16-2745

Published OnlineFirst January 20, 2017; DOI: 10.1158/1078-0432.CCR-16-2745

Translational Relevance

The clinical utility of radionuclide-conjugated bombesin antagonist, currently being investigated in a phase I trial for men with prostate cancer, can be hypothetically augmented by prolonging the radiotracer dwell time within the tumor microenvironment. Here, we test the hypothesis that VTP application in concert with radioisotope delivery can achieve these goals. We show that indeed combination of the 2 treatment modalities improves imaging and delays progression of cancer xenografts compared with ^{90}Y-DOTA-AR monotherapy. Because VTP is in use for localized prostate cancer, the proposed combination may undergo rapid translation to the clinical arena.

VTP is a novel nonthermal ablation approach involving systemic administration of the photosensitizing agent WST-11 (Weizmann STeba-11 drug, Tookad Soluble; Steba Biotech) followed by activation of this agent in the targeted tumor site by laser illumination with near-infrared light (753 nm). Conventional photodynamic therapy (PDT) agents are extravasated to the surrounding tissues mainly affecting the tumor cells (4), whereas WST-11 noncovalently binds to albumin and is sequestered within the circulation, therefore mainly targeting the tumor vasculature until clearance (5, 6). Upon illumination, WST-11 generates reactive oxygen/nitrogen species such as superoxide, hydroxyl radicals, and nitric oxide within the blood vessel that mediate instantaneous arrest of the feeding arteries and draining veins producing an effect similar to profound, localized ischemia/reperfusion injury (6–8). Recent studies have demonstrated that permanent vascular arrest is limited to vessels smaller than 40 μm, which is well-suited to the tumor microenvironment (9). We hypothesized that the ability of WST-11 VTP to permanently shut down the tumor circulation would reduce radiotracer washout from the tumor microenvironment and improve upon localized imaging and treatment effects.

Gastrin-releasing peptide receptor (GRPr; also known as bombesin receptor subtype 2) was shown in a large body of studies to be overexpressed in multiple human cancers at a high incidence rate (10). Specifically, an autoradiographic study of human prostate cancers demonstrated receptor-specific binding of radiolabeled bombesin in all monitored tumors ($n = 30$) as well as in prostatic intraepithelial neoplasia (PIN). In contrast, normal prostate and benign prostate hyperplasia displayed only minimal binding of bombesin (11). As such, a number of radiolabeled bombesin analogs have been developed as targeting vectors for imaging and radionuclide therapy of tumors via specific binding to GRPr (12). Clinical studies with ^{99m}Tc- and ^{68}Ga-labeled bombesin-based peptides have been reported for the imaging of metastasized prostate, breast, and gastrointestinal stromal tumors with high contrast ratios (13–15). Among developed bombesin peptides, ^{111}In-DOTA-AR (a potent bombesin antagonist, ^{111}In-DOTA-PEG$_4$-D-Phe-Gln-Trp-Ala-Val-Gly-His-Sta-Leu-NH$_2$) has demonstrated favorable binding affinities to GRPr and specific uptake in PC-3 human prostate cancer xenografts (16). The optimal uptake of ^{111}In-DOTA-AR was reported to be at 1 to 4 hours postinjection (p.i.) with high tumor-to-background ratios (16). DOTA-AR also allows labeling with therapeutic radioisotopes, such as ^{90}Y ($t_{1/2} = 64$ hours) and ^{177}Lu ($t_{1/2} = 6.73$ days) for radionuclide-based treatment with a rapid accumulation in prostate cancer xenografts. However, about two thirds of delivered radioactivities of both ^{111}In- and ^{90}Y-DOTA-AR are washed out as early as 24 hours p.i. (16, 17), potentially diminishing the therapeutic efficacy. As ^{90}Y is a high-energy beta emitter, which makes it suitable for noninvasive Cerenkov luminescence imaging (CLI), ^{90}Y-DOTA-AR might be the right surrogate to investigate whether the arrest of tumor microvasculature in the target tissue enhances the radiopeptides retention. CLI is a low-cost modality to measure the radioactivity of beta or alpha emitter at multiple time points, and our recent studies showed that there was a linear correlation between the active radiotracer concentrations and CLI signals for ^{90}Y-DOTA-AR in prostate cancer tumor xenografts (17).

To test our hypothesis, we investigated the sequential treatment of prostate cancers with ^{90}Y-DOTA-AR followed by VTP in human xenograft model(s). In this model, we utilized CLI to monitor the retention of the accumulated ^{90}Y-DOTA-AR in the tumor tissues and measured the effects on subsequent tumor growth rate.

Materials and Methods

General

All chemicals were obtained from commercial sources and used without further purification. DOTA-AR, a bombesin antagonist, was synthesized using standard Fmoc strategy (16), and ^{90}Y-DOTA-AR was prepared according to the previously published protocol from our laboratory (17). Radioactivity was measured using an appropriately calibrated dose calibrator (CAPINTEC CRC-30BC). Lyophilized WST-11 was obtained from Steba Biotech. Prostate cancer cell lines, PC-3 and VCaP, were purchased from ATCC. PC-3 cells were maintained in F-12K medium supplemented with 10% FBS, 1.5 g/L sodium bicarbonate, and 2 mmol/L L-glutamine and VCaP in DMEM with high glucose,10% FBS, and 2 mmol/L L-glutamine.

Xenografts

All animal work was performed in accordance with a protocol approved by the IACUC of Memorial Sloan Kettering Cancer Center. To establish prostate tumor xenografts, 5×10^6 PC-3 or VCaP cells resuspended in 150 μL of 1:1 media/Matrigel (BD Biosciences) were inoculated into the shoulder area of athymic nude male mice (6–8 weeks old, NCI, Fredrick, MD). Tumor growth was monitored by caliper measurement twice a week and animal weight was followed as well. When the volume of tumors reached approximately 100 mm^3, the animals were randomly assigned to different cohorts for further experiments.

VTP

WST-11, a photosensitizer, was reconstituted in sterile 5% dextran in water at 2 mg/mL under light-protected condition and the aliquots were stored at −20°C. At the day of VTP treatment, an aliquot was thawed and filtered through 0.2-μm disc syringe filter (Sartorius Stedin Biotech North America). The mice were intravenously injected (bolus for PC-3 xenograft study and infusion for VCaP xenograft study) with WST-11 (9 mg/kg) followed immediately by 10 minutes of laser (Ceramoptec) illumination (755 nm, 150 mW/cm) through a 1-mm frontal fiber (MedLight

Published OnlineFirst January 20, 2017; DOI: 10.1158/1078-0432.CCR-16-2745

S.A.). The light field was arranged to cover the entire tumor area plus 1-mm rim using red-light aiming beam.

CLI

After the mice were anesthetized with isoflurane (1%–4%), the uptake of ^{90}Y-DOTA-AR in xenografts was followed by CLI using the IVIS Spectrum *in vivo* preclinical imaging system (Perkin-Elmer). Images for PC-3 xenografts were captured through 5-minute data acquisition at 3.8–4, 24, 48, 72, 96, and 144 hours postinjection of ^{90}Y-DOTA-AR (14.8 MBq) either with or without VTP application. For quantification of CLI signals, the areas of same size were manually outlined around tumors of *in vivo* images using Living Image 2.60. CL intensity was expressed as average radiance, p/s/cm^2/sr, where number of photons (p) per second (s) per unit surface area (cm^2) per steradian (sr). To determine the effect of VTP on the retention of ^{90}Y-DOTA-AR in another prostate cancer xenografts, mice bearing VCaP tumors were randomly assigned to 2 cohorts for the treatment with ^{90}Y-DOTA-AR alone and ^{90}Y-DOTA-AR/VTP combination. Radiotracer ^{90}Y-DOTA-AR (14.8 MBq) was administered via retro-orbital intravenous injection at 0 hour, and the uptake of ^{90}Y-DOTA-AR was measured with CLI at 3.8 to 4 and 24 hours p.i.

Combination therapy

Mice bearing PC-3 or VCaP xenografts were randomly assigned to 4 different cohorts, including sham control (saline and illumination only), VTP, ^{90}Y-DOTA-AR, and combination of ^{90}Y-DOTA-AR and VTP. Radiotracer ^{90}Y-DOTA-AR (14.8 MBq) was administered via retro-orbital intravenous injection at 0 hour (Fig. 1). Since radiolabeled DOTA-AR displays an optimal tumor uptake at 1 to 4 hours p.i. in GRPr-expressing prostate cancer xenografts (16, 17), we performed VTP treatment at 4 hours p.i. of ^{90}Y-DOTA-AR (Fig. 1). For VTP treatment, WST-11 was injected intravenously followed by laser illumination of tumor area to activate the photosensitizer in tumors. The radioactivities of ^{90}Y-DOTA-AR in the xenografts were quantitatively measured via CLI at 3.8–4 hours p.i. of ^{90}Y-DOTA-AR (for initial uptake prior to VTP) as well as at several later time points. The tumor volume and mouse weights for PC-3 xenografts were monitored one day prior to treatment followed by twice a week until tumor volume approached 1,500 mm^3. The diet and cage for the treated mice were changed every day in the first week of ^{90}Y-DOTA-AR treatment. Organs of interest of sacrificed animals were collected for histologic evaluation.

Radiation dosimetry

On the basis of the CLI data of ^{90}Y-DOTA-AR uptake, the absorbed doses (Gy/MBq) by the PC-3 xenografts were calculated and compared between ^{90}Y-DOTA-AR and ^{90}Y-DOTA-AR/VTP combination treatment groups. CLI was performed at 3.8–4, 24, 48, 72, 96, and 144 hours after ^{90}Y-DOTA-AR administration. The measured photon counts for CLI (p/s/cm^2/sr) were converted to tumor activity using a previously established conversion factor (3.96×10^{-7} MBq/(p/s/cm^2/sr); ref. 17) and subsequently, absorbed radiation dose rate, $r(t)$, was calculated using the equation:

$$r(t) = \Delta\phi A(t)/m(t)$$

In this equation, Δ is the equilibrium dose constant for ^{90}Y (a fixed value of 0.54 g Gy/MBq h); ϕ is a size-dependent value representing the fraction of energy emitted by the tumor taken ^{90}Y; $A(t)$ is the ^{90}Y activity present in the tumor (inferred from the CLI signal and the overall calibration factor); and $m(t)$ is tumor mass (based on caliper measurements, ellipsoidal geometry and an assumed density of 1 g/ml). Absorbed fractions (ϕ) for ^{90}Y were derived by interpolating data published by Bardiès and Chatal (18). Finally, the total absorbed radiation dose to tumor was calculated by numerical integration of dose rate. The integration of dose rate was stopped either at the last measurement time or at the time where the tumor appeared "ablated" (i.e., too small to be measured). Tumors that appeared "ablated" were assigned a nominal size (2 mm diameter sphere) for the purposes of terminal dose rate calculation. Any possible terminal component of dose delivered after the end of integration was ignored.

Histology

Tumors, kidneys, and pancreas were fixed in 10% buffered formalin (Fisher Scientific), embedded in paraffin, sectioned at 5-μm thickness, and stained with hematoxylin and eosin (H&E). Histopathologic analysis to assess tissue toxicity induced by different treatment regimens was performed by a board-certified veterinary pathologist. For immunohistochemical (IHC) analysis of tumor, samples were stained with anti-mouse CD31 antibody (Dianova) to assess tumor vessel density and TUNEL for cell death (19).

Statistical analysis

Data calculated using Microsoft Excel were expressed as mean ± SD. Student unpaired t test (GraphPad Prism 5) was used to determine statistical significance at the 95 % confidence level for ROI analysis and 2-way ANOVA test (GraphPad) for therapeutic efficacy in affecting tumor growth. Differences with $P < 0.05$ were considered to be statistically significant.

Results

Workflow of sequential treatment of xenografts

Depiction of the experimental design is represented in Fig. 1. Tumor xenografts reached size criteria for treatment by 22 to 27 days following implantation. Mice bearing prostate cancer xenografts which express high level of GRPr (PC-3 and VCaP; ref. 17) were used in this study.

In vivo accumulation of ^{90}Y-DOTA-AR in prostate cancer xenografts

PC-3 xenografts. Figure 2A shows a representative CLI of the mice bearing PC-3 xenografts treated with ^{90}Y-DOTA-AR alone (DOTA-AR) and of the ones treated with ^{90}Y-DOTA-AR/VTP combination (combination). Tumors and kidneys are well visualized by CLI as reported by Lohrmann and colleagues (17). Because of the retro-orbital injection of ^{90}Y-DOTA-AR, facial signal was detected occasionally in some mice. After VTP treatment, tumor ablation (eschar formation observed at 144 hours post-VTP) was clearly visible in both VTP (images not shown) and ^{90}Y-DOTA-AR/VTP combination groups (Fig. 2A, 144-hour images in combination panel). High intensity of CLI signals in tumors was observed at 4 hours p.i. of ^{90}Y-DOTA-AR (prior to VTP), and the intensities of signal decreased in a time-dependent manner for both groups. Significantly, CLI displayed enhanced retention of radioactivity for tumors treated with

Published OnlineFirst January 20, 2017; DOI: 10.1158/1078-0432.CCR-16-2745

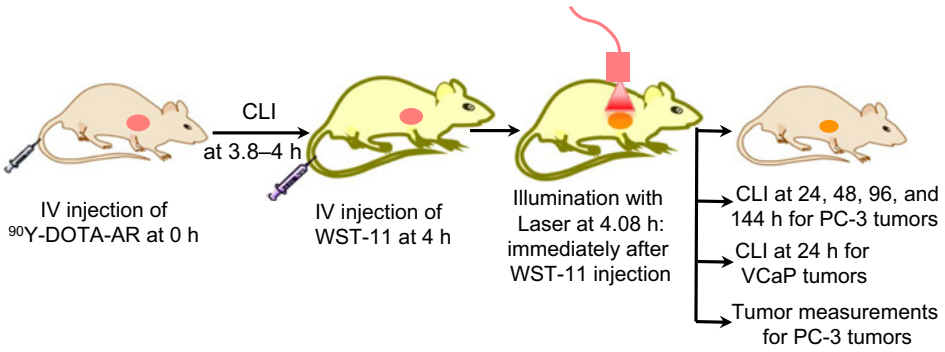

Figure 1.

A workflow for sequential treatments with ^{90}Y-DOTA-AR and VTP in mice with established tumor xenografts. VTP was performed at 4 hours p.i. of ^{90}Y-DOTA-AR intended to trap maximum amount of radioactivity in tumors. The radioactivities of ^{90}Y-DOTA-AR in the xenografts were quantitatively measured via CLI at 3.8–4 hours p.i. for initial uptake radioactivity prior to VTP as well as at 24, 48, 72, 96, and 144 hours p.i. of ^{90}Y-DOTA-AR (PC-3 xenografts) or at 24 hours p.i. of ^{90}Y-DOTA-AR (VCaP xenografts). PC-3 tumor growth was also monitored for antitumor effect of these therapies.

combination therapy compared with tumors treated with ^{90}Y-DOTA-AR alone. Quantitative analysis of ROI with Living Image 2.60 confirmed that PC-3 tumors treated with ^{90}Y-DOTA-AR/VTP combination showed higher radioactivity retention at all time points measured after VTP treatment compared with ^{90}Y-DOTA-AR alone such as 37,000 ± 12,400 and 24,200 ± 9,200 p/s/cm^2/sr, respectively, at 24 hours p.i (Fig. 2B, $P < 0.05$). At 144 hours p.i., there were low but detectable signals at an approximately 1.8-fold higher level in the combination treatment cohort (2,430 ± 426 vs. 1320 ± 142 p/s/cm^2/sr, $P < 0.005$). In contrast, the signal intensities at 4 hours p.i. in the 2 groups (prior to VTP treatment) were similar (92,600 ± 39,100 vs. 91,300 ± 35,300 p/s/cm^2/sr, $P = 0.93$). The half-life of ^{90}Y-DOTA-AR in PC-3 tumors (one-phase decay) was 10.0 ± 0.6 hours in ^{90}Y-DOTA-AR only group and 14.1 ± 0.7 hours in the combination group.

The efficacy of VTP in obliterating tumor vasculature of PC-3 xenografts was assessed via IHC using CD31 marker at 24 hours post-VTP treatment (Fig. 2C). CD31 is the most sensitive and specific endothelial marker in paraffin sections. IHC results with anti-CD31antibody displayed markedly reduced vessel density in PC-3 tumors at 24 hours post-VTP treatment compared with control tumors. In addition, TUNEL stained positive in VTP-treated tumors displaying VTP-induced tumor cell death.

VCaP xenografts. To confirm the general impact of VTP on the enhanced retention of radiopeptide within prostate cancer models, VCaP human prostate cancer xenografts were subjected to the same experimental workflow depicted in Fig. 1. VCaP tumors express high level of GRPr and displayed comparable uptake of ^{90}Y-DOTA-AR to PC-3 xenografts (17). Radioactivity uptake within the VCaP tumors was monitored at 4 and 24 hours p.i. by CLI (Fig. 3). Signal intensities by quantitative ROI analysis for tumors treated with ^{90}Y-DOTA-AR/VTP combination were 2.5-fold higher than for those treated with ^{90}Y-DOTA-AR alone. The difference between groups was statistically significant ($P < 0.05$) at 24 hours p.i. These observations indicate that VTP treatment enhanced retention of delivered radioactivity in both androgen-independent (PC-3) and androgen-dependent (VCaP) prostate cancer xenografts.

Dose estimation of ^{90}Y-DOTA-AR in prostate cancer xenografts

Figure 4 shows the group mean (± SD) values of tumor dose rate as a function of time for the 2 treatment groups. Absorbed doses estimated by integrating these curves were 0.24 (±0.10) Gy/MBq for ^{90}Y-DOTA-AR alone and 0.29 (±0.11) Gy for combination of ^{90}Y-DOTA-AR and VTP. The absorbed dose for the combination was approximately 20% greater and the trend toward higher dose rates becomes clear at later times (≥24 hours p.i.). Absorbed doses (Gy/MBq) for individual PC-3 xenografts were calculated and compared on a group basis between ^{90}Y-DOTA-AR and ^{90}Y-DOTA-AR/VTP combination treatments. The table in Fig. 4B summarizes the statistical data, indicating that both mean and median radiation doses were higher for the combination and when only the radiation dose that was delivered after 24 hours p.i. was considered, the differences were highly significant ($P < 0.01$).

Treatment efficacy in PC-3 xenografts

In vivo PC-3 tumor growth in nude mice was monitored to assess the antitumor effect of ^{90}Y-DOTA-AR or VTP as monotherapy, along with the ^{90}Y-DOTA-AR and VTP combination. Tumor growth up to 34 days posttreatment was followed twice a week, and the individual tumor growth was plotted in Fig. 5A. The control group was sham-treated with laser illumination (without WST-11 administration) and saline injection (i.v.) as a vehicle. A single-dose injection of ^{90}Y-DOTA-AR did not demonstrate statistically significant antitumor effect on tumor growth compared with the control group and did not lead to any tumor regression ($P = 0.97$). This was expected, as we selected a low dose of ^{90}Y-DOTA-AR that had no significant effect on tumor growth on its own to determine any potential synergistic effect of VTP plus radiotherapy. VTP treatment alone had a modest though significant effect on tumor growth compared with control group ($P < 0.01$). However, combination treatment displayed superior efficacy in antitumor effect compared with ^{90}Y-DOTA-AR group ($P < 0.0001$) or VTP group ($P < 0.05$), which indeed suggests a synergistic effect between ^{90}Y-DOTA-AR and VTP. Three of the 12 PC-3 tumor–bearing animals of combination therapy group and 2 of 12 of VTP alone–treated group remained tumor-free at 34 days posttreatment. Figure 5B depicts a superior effect of the combination treatment to ^{90}Y-DOTA-AR single-injection monotherapy.

Published OnlineFirst January 20, 2017; DOI: 10.1158/1078-0432.CCR-16-2745

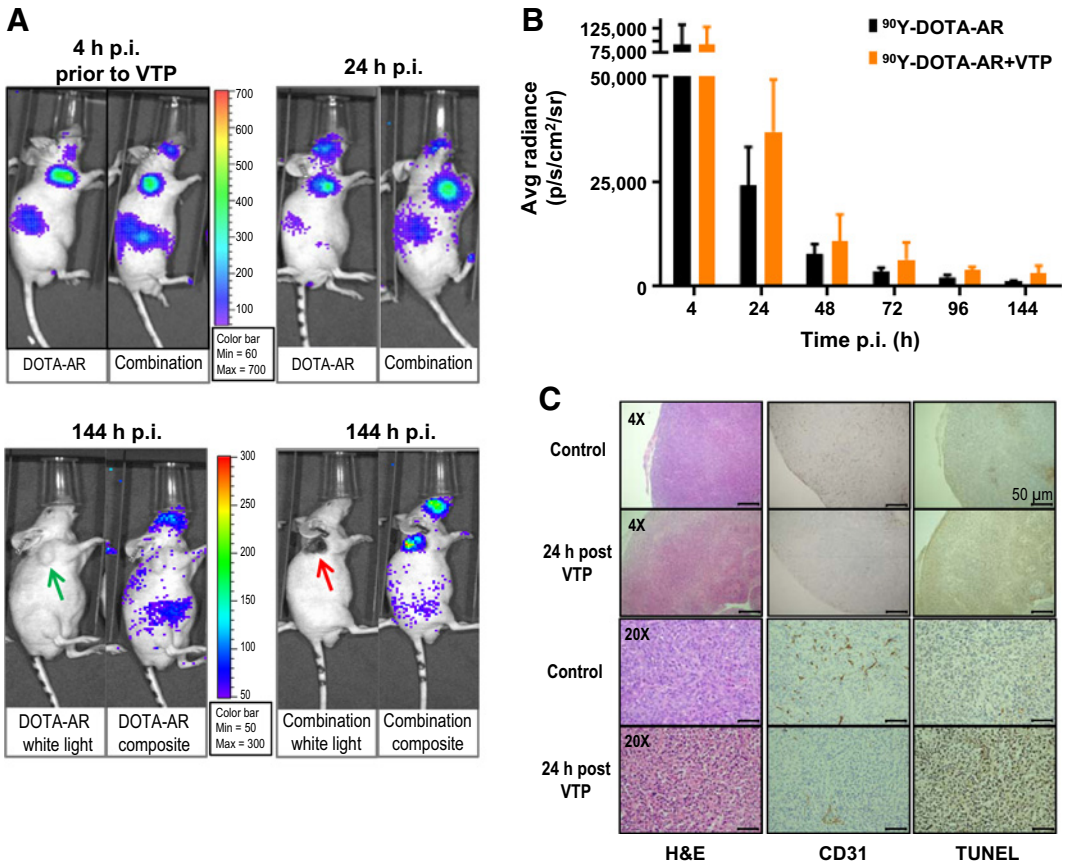

Figure 2.

In vivo CLI of ^{90}Y-DOTA-AR in PC-3 tumor–bearing nude mice. **A,** Representative images of PC-3 xenografts treated with ^{90}Y-DOTA-AR alone (DOTA-AR, $n = 12$) or combination of ^{90}Y-DOTA-AR and VTP (Combination, $n = 13$) at 24 and 144 hours p.i. of ^{90}Y-DOTA-AR. The images at 4 hours p.i. of ^{90}Y-DOTA-AR show the uptake of ^{90}Y-DOTA-AR prior to VTP treatment for both groups. After injection of ^{90}Y-DOTA-AR, the radioactivity uptake within tumor was monitored using the IVIS Spectrum *in vivo* preclinical imaging system. Green arrows = tumor; red arrow = eschar formed posttumor ablation. **B,** ROI analysis of ^{90}Y-DOTA-AR CLI at each time point of imaging. VTP enhanced the retention of ^{90}Y-DOTA-AR radioactivity within the tumors at all the time points measured after VTP treatment ($P < 0.05$). **C,** PC-3 tumors were subjected to H&E staining and IHC of CD31 endothelial marker as well as TUNEL staining. Representative pictures of each group are shown. Tumor vasculature staining with anti-CD31 antibody was significantly reduced at 24 hours post-VTP treatment alone compared with control specimen demonstrating VTP-induced tumor vessel destruction.

Assessment of potential toxic effects of combination therapy

Kidney and pancreas from mice bearing PC-3 tumors in 4 different treatment groups were collected at 41 days posttreatment to investigate potential tissue toxicity caused by ^{90}Y-DOTA-AR/VTP combination therapy. These are the main organs with high level of ^{90}Y-DOTA-AR uptake along with tumors (17). No significant lesions and no evidence of treatment-induced lesions were observed in the kidney and pancreas of these mice (representative H&E pictures in Supplementary Fig. S1). Two mice had minimal focal tubular degeneration and necrosis in kidney: one control mouse and one ^{90}Y-DOTA-AR/VTP–treated mouse. This is a common naturally occurring lesion in experimentally naïve mice.

Discussion

We hypothesized that the local destruction of tumor vessels by VTP may help trap radiotracers in the accumulated organs and thereby improve the clinical outcome of radionuclide-based treatment with beta or alpha emitter–labeled peptide. The current study describes proof-of-principle supporting this hypothesis by demonstrating accumulated ^{90}Y-DOTA-AR in the tumor tissues was retained longer in the prostate cancer xenografts with resultant evidence of improved treatment efficacy from the combination of intratumoral vascular destruction following radiotracer delivery.

CLI as a noninvasive imaging modality

Cherenkov radiation generates visible light as a charged particle emitted from the decaying radioisotope travels through a dielectric medium faster than the speed of light. This visible light can be detected by an optical imaging platform. Several studies found correlations between the light intensities of Cerenkov radiation from different radioisotopes and the energy of particles (20, 21). Among those radionuclides, ^{90}Y produces a high energy of pure beta particle with almost 100% incidence, which allows efficient

Published OnlineFirst January 20, 2017; DOI: 10.1158/1078-0432.CCR-16-2745

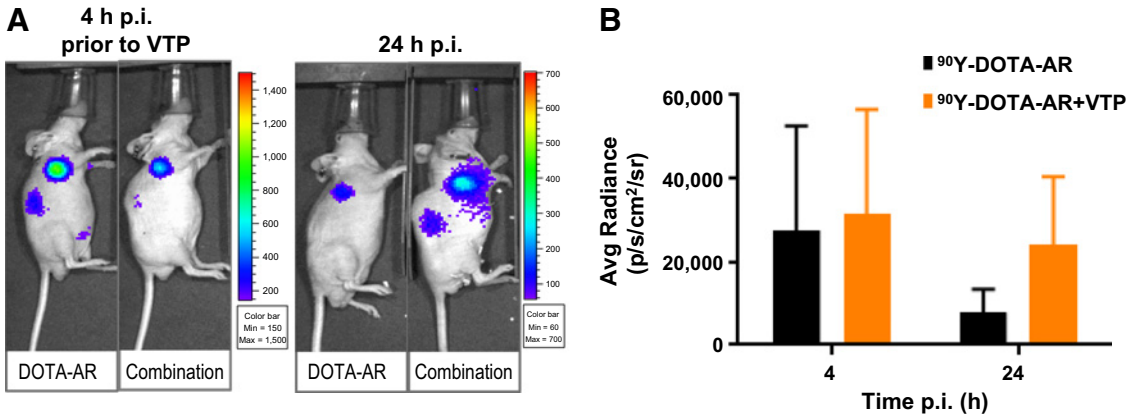

Figure 3.

In vivo CLI of ^{90}Y-DOTA-AR in VCaP tumor–bearing nude mice. **A,** Representative images of VCaP xenografts treated with ^{90}Y-DOTA-AR alone (DOTA-AR) or combination of ^{90}Y-DOTA-AR/VTP (Combination) at 4 and 24 hours p.i. **B,** Graph demonstrates radiance for VCaP at 4 and 24 hours p.i. Tumor uptake of ^{90}Y-DOTA-AR was not significantly different between 2 treatment groups at 4 hours p.i. (prior to VTP, $P = 0.726$, $n = 13$), but a 2.5-fold higher retention of the radioactivity was observed in the tumors of combination group at 24 hours p.i. ($P < 0.0001$, $n = 10$).

measuring of the amount of radioactivity with CLI. Recently, CLI was utilized to quantitatively measure ^{90}Y-DOTA-AR activities in prostate cancer xenografts and kidneys. A strong correlation between radioactivity concentration and *in vivo* CLI intensity ($R^2 = 0.94$–0.98) was observed (17). Therefore, CLI is a reliable, low-cost modality to monitor the retention of ^{90}Y-DOTA-AR radioactivity in a noninvasive way. Our current study further demonstrates that ^{90}Y-DOTA-AR radioactivity in PC-3 xenografts is detectable up to 144 hours p.i. of ^{90}Y-DOTA-AR. Our observations also indicate that CLI could be used to measure the effect of VTP treatment for multiple time points after ^{90}Y-DOTA-AR administration. In addition, most ^{90}Y-DOTA-AR radioactivity was cleared from normal organs within 1 day p.i. as evident by the negligible irradiation dose. This finding is important for the clinical setting where ^{90}Y-DOTA-AR–based CLI is utilized for guiding local therapy.

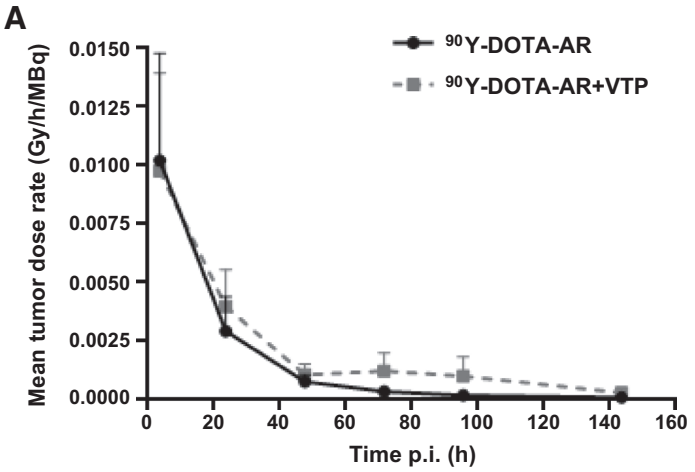

B

Statistics	Absorbed dose (Gy/MBq)			
	^{90}Y-DOTA-AR	^{90}Y-DOTA-AR + VTP	Dose ratio	*P*
Mean (SD) Median (range)	0.24 (0.10) 0.20 (0.10–0.39)	0.29 (0.11) 0.32 (0.09-0.48)	1.2 1.6	0.25
Mean 24 (SD) Median 24 (range)	0.07 (0.03) 0.07 (0.03–0.12)	0.12 (0.04) 0.11 (0.15–0.19)	1.6 1.6	0.005

Figure 4.

Estimated absorption dose of ^{90}Y-DOTA-AR in PC-3 xenografts. **A,** Estimated dose ratio between ^{90}Y-DOTA-AR and combination of ^{90}Y-DOTA-AR/VTP is depicted. **B,** Table shows the summary statistics for both treatment groups. Both mean and median radiation doses were higher for ^{90}Y-DOTA-AR and VTP. The number 24 denotes radiation dose delivered ≥24 hours p.i.

Published OnlineFirst January 20, 2017; DOI: 10.1158/1078-0432.CCR-16-2745

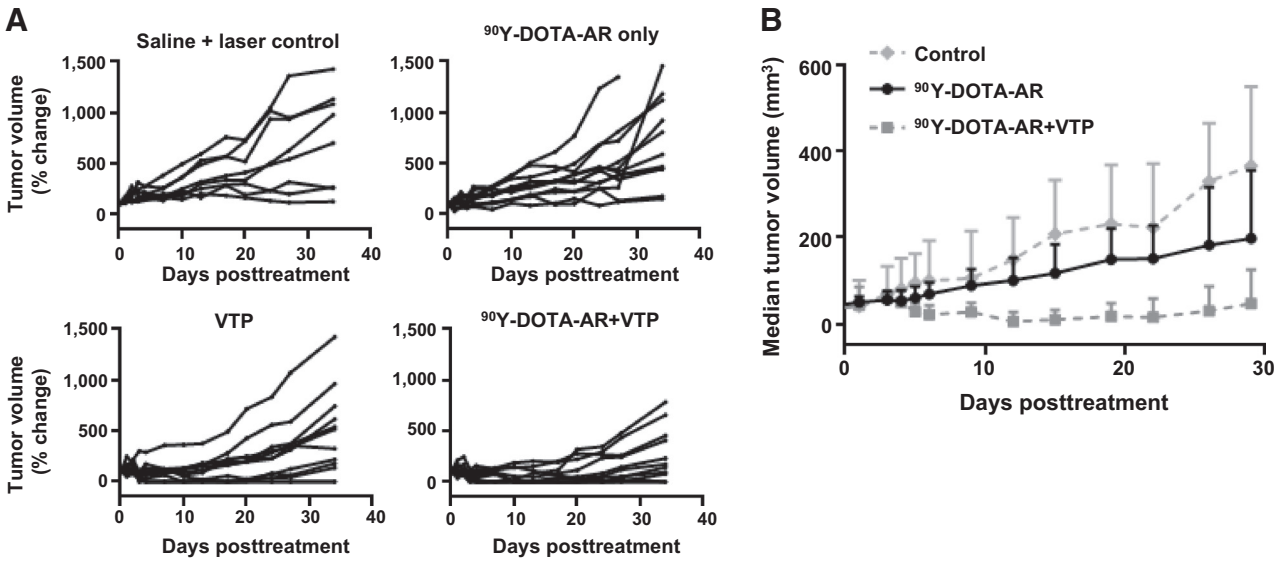

Figure 5.

Therapeutic efficacy of VTP, ^{90}Y-DOTA-AR, and ^{90}Y-DOTA-AR/VTP combination on PC-3 xenografts. **A,** Individual tumor growth per each cohort is shown. Mice bearing PC-3 xenografts were randomly assigned to 4 different cohorts of sham control (saline and illumination only, $n = 8$), VTP ($n = 12$), ^{90}Y-DOTA-AR ($n = 12$), and combination of ^{90}Y-DOTA-AR and VTP ($n = 13$). ^{90}Y-DOTA-AR alone did not demonstrate statistically significant antitumor effect on tumor growth ($P = 0.97$), whereas VTP treatment alone had a modest effect on tumor growth compared with control group ($P < 0.01$). Combination treatment displayed statistically significant antitumor effect compared to ^{90}Y-DOTA-AR alone arm ($P < 0.0001$) or to VTP alone arm ($P < 0.05$) suggesting synergy between radiotherapy and VTP. Two-way ANOVA test was utilized for the statistical analysis. **B,** Graph shows the median tumor volume as a function of time. This shows a clear demarcation between treatment groups with the combination of ^{90}Y-DOTA-AR plus VTP having a much more pronounced therapeutic effect.

Combination with VTP to increase tumor retention time of the accumulated radioactivity

This study demonstrates the potential for utilization of VTP as a means to augment the activity of radiotracers within tumors. The combinational strategy significantly increased intratumoral lifetime of radiopharmaceuticals in androgen-independent PC-3 human prostate cancer xenografts monitored by CLI ($P < 0.05$ in all time points post-VTP). The radioactivity in combination cohort was approximately 1.5-fold higher in this model with approximately 40% increase of ^{90}Y-DOTA-AR half-life in tumors treated with VTP. Even higher retention of radioactivity in combination with VTP (2.5-fold) compared with radiotracer delivery alone was observed in androgen-dependent VCaP human prostate cancer xenograft model as well, indicating broad applicability of this approach. Our models also, however, suggested slight differences in the degree of radioactivity retention between tumor types, the cause for which is unclear. This could be variability within the experimental design or related to biologic differences in tumor microenvironment related to vascularity or radiotracer uptake. VTP targets tumor microvasculature exclusively affecting both small feeding arterioles and draining venules (8). Our preliminary histologic analysis did not identify obvious vascular differences, yet more detailed studies could provide greater insight.

The longer retention of intratumoral radioactivity observed in combination cohorts nicely correlated to the treatment efficacy of PC-3 tumors (Fig. 5). This is especially striking when noting that, compared to controls, ^{90}Y-DOTA-AR alone did not demonstrate any antitumor effect on tumor growth. However, the combination treatment displayed significant antitumor effects compared with both ^{90}Y-DOTA-AR alone and VTP alone, suggesting a synergistic effect between 2 modalities.

Analysis of radiation dose rates and total doses in the PC-3 tumors indicated that VTP produced an enhancement that was statistically significant for times $\geq$24 hours p.i. of radiotracer or approximately $\geq$20 hours after VTP treatment (Fig. 4). Radiotracer concentration was not significantly influenced before this time point, although this phase of washout is fairly rapid with more variability seen in measurements over this interval likely reflected in differences in tracer clearance. Still, it is possible that adaptations in the approach might positively influence radioactivity accumulation in tumors at earlier time points. Multiple dosing of radiotracer and a shorter interval than 4 hours between the administration of radiotracer and VTP treatment are modifications that could be tried to achieve VTP-induced vascular breakdown, whereas tumor uptake of radiotracer is less prone to washout. Alternatively, VTP treatment parameters could be altered to increase the degree of intratumoral vascular destruction or that of surrounding vessels that may reduce the amount of ^{90}Y-DOTA-AR activity exiting from the tumors. Dose-escalation studies of VTP parameters such as WST-11 concentration or/and laser fluence should provide better efficacy of VTP for the combination with ^{90}Y-DOTA-AR. Preclinical large animal studies of VTP and multicenter phase II and III studies of localized prostate cancer have reported a dose-dependent response rate that depends on the treatment conditions of WST-11 concentration and laser fluence (22–25). Further evaluation of these factors may be warranted.

Several clinical applications for this form of therapy are conceivable. Published trial data in localized prostate cancer have

Published OnlineFirst January 20, 2017; DOI: 10.1158/1078-0432.CCR-16-2745

demonstrated excellent safety and tolerability for WST-11 VTP treatment within the pelvis without injury to surrounding, highly sensitive organs. Effective local tumor ablation is also impressive, with absent evidence of cancer in 80% of cases. Causes for the few local failures have not been elucidated; however, combinatorial treatment with ^{90}Y-DOTA-AR could be a means to improve upon these results, particularly in high-risk cancers. Other difficult-to-treat sites in soft tissue might also be amenable as in the case of local or regional recurrence after prior surgery or radiation. Studies in bone metastases remain to be performed, although vascular dynamics in this compartment may influence the dynamics of treatment with this approach and establishing reliable preclinical models in this setting are a challenge requiring further refinement.

This study reports on the initial experience with combinatorial sequential therapy using VTP with radiopharmaceutical therapy demonstrating highly promising results that have potential to improve upon cytotoxic effects in prostate cancers. As VTP therapy does not result in serious phototoxicity and its interval between drug injection and laser illumination is short, it provides an attractive option to overcome limitations of fast washout of the accumulated radiopharmaceuticals from tumors. The experiments presented here constitute a proof-of-principle for the use of combined radionuclide/VTP strategies that may be further developed and eventually translated into clinical studies.

Disclosure of Potential Conflicts of Interest

A. Scherz is listed as an inventor on a patent regarding WST11, which is owned by the Weizmann Institute commercial branch "Yeda" and licensed to Steba-Biotech. W.A. Weber reports receiving commercial research grants from Piramal. No potential conflicts of interest were disclosed by the other authors.

Authors' Contributions

Conception and design: K. Kim, H. Zhang, A. Scherz, W.A. Weber, J.A. Coleman
Development of methodology: K. Kim, H. Zhang, S. La Rosa, A. Scherz, J.A. O'Donoghue, W.A. Weber, J.A. Coleman
Acquisition of data (provided animals, acquired and managed patients, provided facilities, etc.): K. Kim, H. Zhang, S. Jebiwott, P. Desai, S. Kimm
Analysis and interpretation of data (e.g., statistical analysis, biostatistics, computational analysis): K. Kim, H. Zhang, S. La Rosa, P. Desai, A. Scherz, J.A. O'Donoghue, W.A. Weber, J.A. Coleman
Writing, review, and/or revision of the manuscript: K. Kim, H. Zhang, A. Scherz, J.A. O'Donoghue, W.A. Weber, J.A. Coleman
Administrative, technical, or material support (i.e., reporting or organizing data, constructing databases): K. Kim, H. Zhang, S. La Rosa, P. Desai, S. Kimm
Study supervision: K. Kim, A. Scherz, W.A. Weber, J.A. Coleman

Acknowledgments

The authors thank MSKCC Small Animal Imaging Core Facility.

Grant Support

This work was supported by NIH grant P50-CA84638 (H. Zhang, W.A. Weber), Thompson Family Foundation (K. Kim, S. La Rosa, S. Jebiwott, S. Kimm, A. Scherz, J.A. Coleman), and NIH Small-Animal Imaging Research Program grant R24 CA83084 and NIH Center grant (P30 CA08748). H. Zhang was additionally supported by CURE Childhood Cancer Foundation.

The costs of publication of this article were defrayed in part by the payment of page charges. This article must therefore be hereby marked *advertisement* in accordance with 18 U.S.C. Section 1734 solely to indicate this fact.

Received October 31, 2016; revised December 19, 2016; accepted January 4, 2017; published OnlineFirst January 20, 2017.

References

1. Reubi JC.Peptide receptors as molecular targets for cancer diagnosis and therapy. Endocr Rev 2003;24:389–427.
2. Ambrosini V, Fani M, Fanti S, Forrer F, Maecke HR. Radiopeptide imaging and therapy in Europe. J Nucl Med 2011;52:42S–55S.
3. Graham MM, Menda Y. Radiopeptide imaging and therapy in the United States. J Nucl Med 2011;52:56S–63S.
4. Juarranz A, Jaén P, Sanz-Rodríguez F, Cuevas J, González S. Photodynamic therapy of cancer. Basic principles and applications. Clin Transl Oncol 2008;10:148–54.
5. Vakrat-Haglili Y, Weiner L, Brumfeld V, Brandis A, Salomon Y, McLlroy B, et al. The microenvironment effect on the generation of reactive oxygen species by Pd-bacteriopheophorbide. J Am Chem Soc 2005;127:6487–97.
6. Mazor O, Brandis A, Plaks V, Neumark E, Rosenbach-Belkin V, Salomon Y, et al. WST11, a novel water-soluble bacteriochlorophyll derivative; cellular uptake, pharmacokinetics, biodistribution and vascular-targeted photodynamic activity using melanoma tumors as a model. Photochem Photobiol 2005;81:342–51.
7. Gross S, Gilead A, Scherz A, Neeman M, Salomon Y. Monitoring photodynamic therapy of solid tumors online by BOLD-contrast MRI. Nat Med 2003;9:1327–31.
8. Madar-Balakirski N, Tempel-Brami C, Kalchenko V, Brenner O, Varon D, Scherz A, et al. Permanent occlusion of feeding arteries and draining veins in solid mouse tumors by vascular targeted photodynamic therapy (VTP) with Tookad. PLoS One 2010;5:e10282.
9. Kimm SY, Tarin TV, Monette S, Srimathveeravalli G, Gerber D, Durack JC, et al. Nonthermal ablation by using intravascular oxygen radical generation with WST11: dynamic tissue effects and implications for focal therapy. Radiology 2016; 281:109–18.
10. Reubi JC, Wenger S, Schmuckli-Maurer J, Schaer JC, Gugger M. Bombesin receptor subtypes in human cancers: detection with the universal radioligand (125)I-[D-TYR(6), beta-ALA(11), PHE(13), NLE(14)] bombesin (6-14). Clin Cancer Res 2002;8:1139–46.
11. Markwalder R, Reubi JC. Gastrin-releasing peptide receptors in the human prostate: relation to neoplastic transformation. Cancer Res 1999;59:1152–9.
12. Sturzu A, Sheikh S, Echner H, Nagele T, Deeg M, Amin B, et al. Rhodamine-marked bombesin: a novel means for prostate cancer fluorescence imaging. Invest New Drugs 2014;32:37–46.
13. Mansi R, Fleischmann A, Macke HR, Reubi JC. Targeting GRPR in urological cancers-from basic research to clinical application. Nat Rev Urol 2013; 10:235–44.
14. Mather SJ, Nock BA, Maina T, Gibson V, Ellison D, Murray I, et al. GRP receptor imaging of prostate cancer using [(99m)Tc]Demobesin 4: a first-in-man study. Mol Imaging Biol 2014;16:888–95.
15. Kahkonen E, Jambor I, Kemppainen J, Lehtio K, Gronroos TJ, Kuisma A, et al. *In vivo* imaging of prostate cancer using [Ga]-labeled bombesin analog BAY86-7548. Clin Cancer Res 2013;19:5434–43.
16. Abiraj K, Mansi R, Tamma ML, Fani M, Forrer F, Nicolas G, et al. Bombesin antagonist-based radioligands for translational nuclear imaging of gastrin-releasing peptide receptor-positive tumors. J Nucl Med 2011;52:1970–78.
17. Lohrmann C, Zhang H, Thorek DL, Desai P, Zanzonico PB, O'Donoghue J, et al. Cerenkov luminescence imaging for radiation dose calculation of a 90Y-labeled gastrin-releasing peptide receptor antagonist. J Nucl Med 2015;56: 805–11.
18. Bardies M, Chatal JF. Absorbed doses for internal radiotherapy from 22 beta-emitting radionuclides: beta dosimetry of small spheres. Phys Med Biol 1994;39:961–81.
19. Gavrieli Y, Sherman Y, Ben-Sasson SA. Identification of programmed cell death in situ via specific labeling of nuclear DNA fragmentation. J Cell Biol 1992;119:493–501.
20. Thorek D, Robertson R, Bacchus WA, Hahn J, Rothberg J, Beattie BJ, et al. Cerenkov imaging- anew modality for molecular imaging. Am J Nucl Med Mol Imaging 2012;2:163–73.

Published OnlineFirst January 20, 2017; DOI: 10.1158/1078-0432.CCR-16-2745

21. Das S, Thorek DL, Grimm J. Cerenkov imaging. Adv Cancer Res 2014; 124:213–34.
22. Kimm SY, Tarin TV, Monette S, Srimathveeravalli G, Gerber D, Durack JC, et al. Nonthermal ablation by using intravascular oxygen radical generation with WST11: dynamic tissue effects and implications for focal therapy. Radiology 2016;281:109–18.
23. Murray KS, Winter AG, Corradi RB, LaRosa S, Jebiwott S, Somma A, et al. Treatment effects of WST11 vascular targeted photodynamic therapy for urothelial cell carcinoma in swine. J Urol 2016;196:236–43.
24. Azzouzi AR, Barret E, Bennet J, Moore C, Taneja S, Muir G, et al. TOOKAD® Soluble focal therapy: pooled analysis of three phase II studies assessing the minimally invasive ablation of localized prostate cancer. World J Urol 2015;33:945–53.
25. Azzouzi AR, Barret E, Moore CM, Villers A, Allen C, Scherz A, et al. TOOKAD® Soluble vascular-targeted photodynamic (VTP) therapy: determination of optimal treatment conditions and assessment of effects in patients with localised prostate cancer. BJU Int 2013;112: 766–74.

AACR American Association for Cancer Research

Clinical Cancer Research

Bombesin Antagonist-Based Radiotherapy of Prostate Cancer Combined with WST-11 Vascular Targeted Photodynamic Therapy

Kwanghee Kim, Hanwen Zhang, Stephen La Rosa, et al.

Clin Cancer Res Published OnlineFirst January 20, 2017.